

Darbepoetin- α inhibits the perpetuation of necro-inflammation and delays the progression of cholestatic fibrosis in mice

Michael Sigal, Nikolai Siebert, Dietmar Zechner, Elena Menschikow, Kerstin Abshagen, Brigitte Vollmar and Christian Eipel

Biliary obstruction and cholestasis result in hepatocellular necro-inflammation and lead to the development of liver fibrosis. The objective of this study was to analyze whether the multiple tissue-protective properties of erythropoietin are salutary in an experimental model of liver fibrosis. For this purpose, C57BL/6J mice underwent common bile duct ligation (BDL) and were treated with either darbepoetin- α (10 μ g/kg i.p.) or physiological saline every third day, beginning 24 h after BDL. Mice were killed at 2, 5, 14, and 28 days after BDL. Beside hematological parameters, markers of inflammation and fibrosis were assessed histomorphometrically and immunohistochemically as well as by quantitative real-time PCR. In addition, a 7-week survival study was performed. BDL provoked cholestatic hepatitis characterized by biliary infarcts with accumulation of macrophages followed by marked collagen deposition and increased expression of profibrotic gene transcripts. Darbepoetin- α treatment significantly diminished the area of focal necrosis, reduced the infiltration of macrophages, decreased levels of profibrotic genes, and lowered collagen deposition. Moreover, darbepoetin- α significantly reduced systemic anemia caused by BDL. Finally, darbepoetin- α treatment significantly prolonged the survival time after BDL. This study suggests that darbepoetin- α , which is a clinically well-established substance, might be used as an efficient therapeutic option for patients with chronic cholestatic liver disease.

Laboratory Investigation (2010) 90, 1447–1456; doi:10.1038/labinvest.2010.115; published online 21 June 2010

KEYWORDS: bile duct ligation; erythropoietin; hypoxia-inducible factor; liver; survival

Obstruction of the bile duct or extrahepatic cholestasis occurs in humans in a variety of clinical settings, such as gallstone impaction, cholangiocarcinoma, extrinsic compression by tumors or enlarged lymph nodes, and sclerosing cholangitis.^{1,2} Cholestasis results in the retention of hydrophobic bile acids in the liver, inflammation as well as hepatocellular necrosis, leading to the development of liver fibrosis.^{3,4} Fibrogenesis is initiated when liver injury stimulates cells to synthesize and secrete growth factors, especially transforming growth factor- β (TGF- β), that activates hepatic stellate cells and other cell types, such as peribiliary fibroblasts, to produce collagen.⁵ One of the mechanisms by which liver injury stimulates the production of growth factors is hepatocellular hypoxia. Recently, Moon *et al*⁶ reported that hypoxia-inducible factor (HIF)-1 α is a critical regulator of profibrotic mediator production during the development

of liver fibrosis. In line with this, many studies have reported a relationship between hypoxia and liver fibrosis in different experimental models.^{6–8}

The renal glycoprotein hormone erythropoietin (Epo) has been well characterized as a primary mediator of the normal physiological response to hypoxia. Recombinant human Epo and its longer-acting hyperglycosylated analog, darbepoetin- α (DPO), are used to treat anemia associated with chronic diseases and non-myeloid cancer.⁹ However, Epo also ameliorates acute and chronic injury in several organs by its pleiotropic tissue-protective effects. Recent studies have identified multiple functions of Epo and DPO that coordinate local responses to injury by attenuating both apoptotic and necrotic cell death.^{9,10} Consistent with these findings, our group has recently reported the protective effects of DPO in mice with septic liver failure.¹¹ As it is not

Institute for Experimental Surgery, University of Rostock, Rostock, Germany

Correspondence: Dr C Eipel, PhD, Institute for Experimental Surgery, University of Rostock, 18055 Rostock, Germany.

E-mail: christian.eipel@uni-rostock.de

Received 4 November 2009; revised 3 May 2010; accepted 18 May 2010

known whether the pleiotropic properties of DPO are beneficial in treatment of cholestatic liver injury, we aimed to examine whether DPO exerts an antifibrotic effect on a mouse model of common bile duct ligation (BDL). We further assessed the hypothesis that DPO administration improves survival after BDL.

MATERIALS AND METHODS

Mice

Male C57BL/6J mice were purchased from Charles River Laboratories (Sulzfeld, Germany) and were used at 8–10 weeks of age with a body weight of 23–26 g. Animals were kept on water and standard laboratory chow *ad libitum*. The experiments were conducted in accordance with the German legislation on protection of animals and the NIH Guide for the Care and Use of Laboratory Animals (Institute of Laboratory Animal Resources, National Research Council).

Surgical Procedure and Experimental Groups

Mice were anesthetized with isoflurane. BDL was performed after midline laparotomy. The common bile duct was ligated three times with 5-0 silk and transected between the two most distal ligations. Sham operation was performed similarly except for ligation and transection of the bile duct ($n = 6$). A total of 60 BDL mice were randomized into two groups. Darbepoetin- α (10 $\mu\text{g}/\text{kg}$ body weight, Aranesp; Amgen Europe, Breda, The Netherlands) or the same volume of isotonic saline was injected intraperitoneally in a blinded manner every third day, beginning at the first day after BDL. This therapeutic schedule was adapted from the study of Sasu *et al*,¹² comparing the biological activity of epoetin- α and darbepoetin- α under different administration schedules in mice. To obtain blood and liver samples, mice (10 animals per group at each time point) were killed at days 2 and 5 as early time points for evaluation of hepatocellular necrosis and inflammation or at days 14 and 28 after BDL for evaluation of fibrosis. These time points were chosen in accordance with a recently published study describing the time-related changes after BDL in C57BL/6J mice.¹³

Hematological Measurements and Plasma Enzyme Levels

Animals were anesthetized and exsanguinated by puncture of the vena cava inferior. Red blood cell count, hemoglobin, and hematocrit were assessed with an automated cell counter (Sysmex KX-21, Sysmex). Plasma activity of alanine aminotransferase (ALT) was measured spectrophotometrically as marker of hepatocellular desintegrity, and plasma concentration of total bilirubin served as parameter of cholestasis.

Histopathology and Image Analysis

Liver tissue samples were fixed in formalin for 2 to 3 days and embedded in paraffin. Sections (5 μm) were stained with hematoxylin and eosin (H&E) for routine examination and

quantification of bile infarcts. Sirius-red-stained sections served for quantification of collagen deposition. All samples from a series of experiments were stained simultaneously and evaluated in a blinded manner. For histomorphometric analysis, images of 20 random low-power fields ($\times 10$ magnification, Olympus BX 51, Hamburg, Germany) were acquired with a Color View II FW camera (Color View, Munich, Germany) and evaluated using an image analysis system (Adobe Photoshop, Adobe Systems, Uxbridge, UK). Fibrosis deposition was quantified as a percentage of Sirius-red-stained area compared with the total section area. The surfaces of large centrilobular veins and large portal tracts were excluded from this calculation. Bile infarcts were quantified in H&E-stained sections in a similar manner and the percentage of the focal necrosis surface to the total liver section area was assessed.

Immunohistochemistry

To evaluate the cellular inflammatory response, the numbers of resident liver macrophages were analyzed using the F4/80 antigen (1:10; Serotec, Oxford, UK). Overnight incubation (4 °C) with the first antibody (polyclonal rat anti-F4/80) was followed by conjugated mouse anti-rat immunoglobulin (1:200; Santa Cruz Biotechnology, Santa Cruz, CA, USA). The sites of alkaline phosphatase binding were detected using the chromogen fuchsin (Dako Cytomation, Hamburg, Germany).

For HIF-1 α analysis, sections were incubated overnight at 4 °C with rabbit polyclonal anti-HIF-1 α antibody (1:100; Santa Cruz). After equilibrating to room temperature, sections were incubated with a horseradish peroxidase-conjugated secondary antibody according to the manufacturer's instructions (Dako Cytomation). As chromogen, 3-amino-9-ethylcarbazole substrate (Dako Cytomation) was used, which forms a red end product at the site of the target antigen.

Real-Time PCR

Total RNA from liver tissue was isolated using RNeasy mini kit (Qiagen, Germany) according to the manufacturer's instructions. Total RNA was eluted in 30 μl of nuclease-free water, quantified spectrophotometrically at 260 nm, and kept at -80 °C until use. First-strand cDNA was synthesized by reverse transcription of 2 μg of total RNA using oligo(dT) 18 primer (Biolabs, Frankfurt am Main, Germany) and Superscript II RNaseH-Reverse Transcriptase (Invitrogen, Karlsruhe, Germany) in the presence of dNTPs, 5 \times first-strand buffer, and dithiothreitol at 72 °C for 10 min and 42 °C for 60 min. The reverse transcriptase was inactivated at 95 °C for 5 min. Expression levels of murine collagen-(I)- $\alpha 1$, CRP2 (cysteine- and glycine-rich protein 2), α -SMA, and TGF- $\beta 1$ mRNA were quantified relative to control samples (LightCycler System 1.5; Roche, Mannheim, Germany) and normalized to the expression of the housekeeping gene *GAPDH*. For our approach, we used SYBR Green I (Roche) for the detection of dsDNA amplified in the PCR. Primers used for all real-time PCR experiments are listed in Table 1.

Primers were designed spanning introns to eliminate false-positive signals from contaminating genomic DNA as well as to anneal at approximately 55 °C to combine both reactions of GAPDH and target gene in the same run. The real-time PCR program included a 10-min denaturation step followed by 40–50 amplification cycles. After each LightCycler run, a melting curve analysis was performed to analyze the products of the PCR. LightCycler PCR products were separated once by 1% agarose (peqGOLD Universal Agarose; peqLab Biotechnologie, Erlangen, Germany) gel electrophoresis containing 0.5 µg/ml ethidium bromide to confirm the right amplification products. For the quantification of gene expression, duplicates were run in the LightCycler for both genes. The reaction without cDNA template was also performed as a negative control.

Survival Study

For assessment of survival, additional 20 animals underwent BDL and were treated in a blinded manner either with saline

(10 µl/g body weight) or with darbepoetin in the same concentration and frequency as described above ($n = 10$ per group). The clinical status of the mice was examined every day and cases of death were noted. The survival study was terminated at 49 days after BDL.

Statistics

Data were presented as mean ± s.e.m. After performing normality test, statistical differences between the two BDL groups were determined using *t*-test. Mann–Whitney rank-sum test was used if criteria for parametric tests were not met. Multiple comparisons were performed by analysis of variance followed by the appropriate *post hoc* comparison test. Furthermore, for analysis of survival data, Kaplan–Meier survival analysis was applied followed by the log-rank test. Data were considered significant when $P < 0.05$. Statistical analysis was performed using the Sigma Stat and Sigma Plot software package (Jandel Scientific, San Rafael, CA, USA).

RESULTS

Darbeopetin Reduces BDL-Induced Anemia and HIF-1 α Expression in the Fibrotic Liver

Chronic liver diseases are associated with systemic hypoxemia through loss of red blood cells, leading to an overexpression of different factors, such as HIF-1 α , which cause fibrogenesis.⁶ At 14 days after BDL, animals showed a significant reduction in hematocrit, red blood cells, and hemoglobin as shown in Figure 1. DPO reduced the drop of hemoglobin, resulting in less severe anemia. Furthermore, the application of DPO reduced the overexpression of HIF-1 α in bile infarcts and fibrotic areas (Figure 2, right column).

Darbeopetin Ameliorates Hepatocellular Injury, Inflammation, and Cholestasis in BDL Mice

To investigate the degree of hepatocellular injury after BDL, serum activity of ALT was measured and histological

Table 1 Primers used for real-time PCR

Gene	Primer	Sequence	Product size
α -SMA	Forward	5'-ACTACTGCCGAGCGTGAGAT-3'	452 bp
	Reverse	5'-AAGGTAGACAGCGAAGCCAG-3'	
collagen-(I)-1 α	Forward	5'-GAAACCCGAGGTATGCTTGA-3'	276 bp
	Reverse	5'-GACCAGGAGGACCAGGAAGT-3'	
TGF- β 1	Forward	5'-CCAGATCTCTCCAAACTAA-3'	344 bp
	Reverse	5'-GCTCCACAGTTGACTTGAAT-3'	
CRP2	Forward	5'-GCTACGGAAAGAAGTATGGACC-3'	299 bp
	Reverse	5'-CTCAGTCAGAGTTGTAGACTCC-3'	
GAPDH	Forward	5'-AACGACCCCTTCATTGAC-3'	191 bp
	Reverse	5'-TCCACGACATACTCAGCAC-3'	

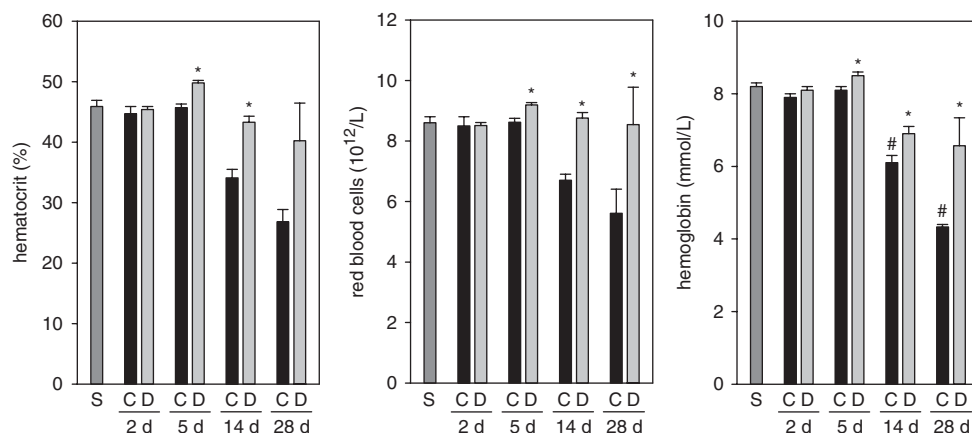


Figure 1 Hematocrit (left), red blood cell count (middle), and hemoglobin concentration (right) in sham-operated mice (S) ($n = 6$) and in animals at 2, 5, 14, and 28 days after BDL with administration of either 10 µg/kg body weight darbepoetin- α (D) or physiological saline (C) every third day, beginning 24 h after surgery ($n = 10$ per group and time point). Data are given as mean ± s.e.m. # $P < 0.05$ versus sham (S); * $P < 0.05$ versus control (C) at the respective time points.

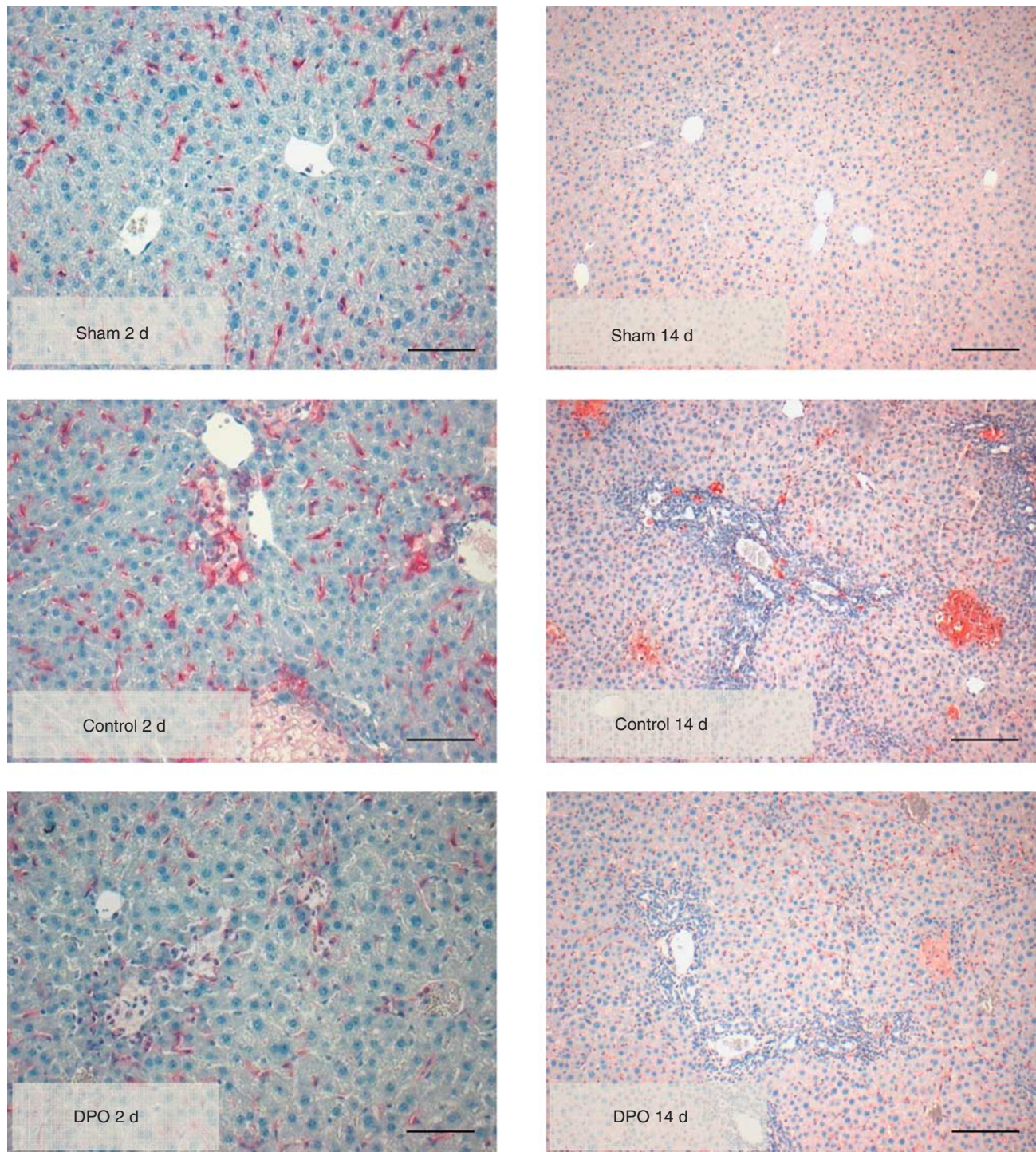


Figure 2 Representative immunohistochemical images of F4/80 antigen in liver tissue sections (left column) of a sham-operated animal (Sham 2 d), a saline-treated control (Control 2 d), and a DPO-treated animal (DPO 2 d) at 2 days after BDL (bar represents 50 μm). Right column shows immunohistochemical images of HIF-1 α in liver tissue sections of a sham-operated animal (Sham 14 d), saline-treated control (Control 14 d), and a DPO-treated animal (DPO 14 d) at 14 days after BDL (bar represents 100 μm).

quantification of biliary infarcts was performed. ALT activity markedly increased after BDL as a sign of hepatocellular disintegration (Figure 3, left). Treatment with DPO markedly reduced ALT release in particular at days 2 and 28 after BDL. Total bilirubin concentration increased in plasma of BDL

mice, reaching a maximum at 14 days. Administration of DPO significantly reduced bilirubin levels at day 2 when compared with saline-treated controls (Figure 3, right). Histomorphometric analysis of biliary infarcts in liver tissue, defined as clusters of injured hepatocytes, revealed a

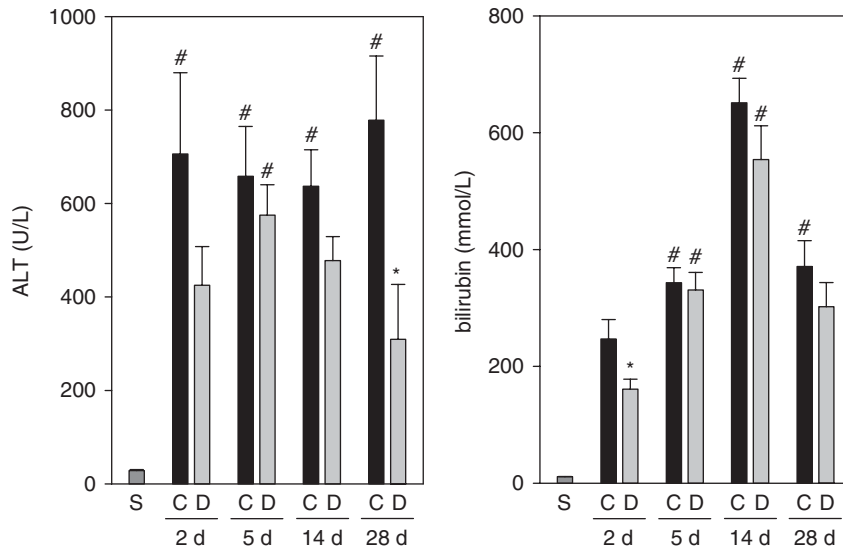


Figure 3 Plasma activity of ALT (left) and concentration of bilirubin (right) in sham-operated mice (S) ($n=6$) and in animals at 2, 5, 14, and 28 days after BDL with administration of either 10 $\mu\text{g}/\text{kg}$ body weight darbepoetin- α (D) or physiological saline (C) every third day, beginning 24 h after surgery ($n=10$ per group and time point). Data are given as mean \pm s.e.m. $\#P<0.05$ versus sham (S); $*P<0.05$ versus control (C) at the respective time points.

significant reduction in the area of focal necrosis by DPO treatment at both days 2 and 14 after BDL (Figure 4). To investigate whether these biliary infarcts trigger the inflammatory reaction, we performed immunohistochemistry of the F4/80 antigen. The number of F4/80-positive macrophages was excessively increased around the focal infarcts in saline-treated BDL mice (Figure 2, left column). DPO markedly attenuated the inflammatory reaction with almost the same distribution and number of macrophages as observed in sham-treated animals. These data show the antinecrotic and anti-inflammatory potential of DPO in the process of cholestasis.

Darbepoetin Delays the Progression of BDL-Induced Fibrosis

Liver sections of mice at day 14 after surgery showed a significant increase in Sirius-red-stained collagen fibers, especially around the portal regions (Figure 5). In DPO-treated mice, Sirius-red-positive staining was slightly decreased, but was statistically significant, implicating some antifibrotic property of DPO (Figure 5). No further elevation of Sirius-red-positive area was observed at day 28 after BDL compared with day 14, with a small but statistically not different decrease in DPO-treated mice at 28 days after BDL.

Darbepoetin Affects Fibrosis-Associated Gene Expression

Real-time PCR was used to determine the expression of markers of fibrosis, such as collagen-(I)- $\alpha 1$, α -SMA, CRP2, and TGF- $\beta 1$. Consistent with the histological evaluations, expression of collagen-(I)- $\alpha 1$ mRNA steadily increased after BDL. DPO treatment caused a significant reduction in collagen-(I)- $\alpha 1$ mRNA levels at days 2 and 14 compared with

the saline-treated controls (Figure 6). In addition, we evaluated the expression levels of CRP2 mRNA, a marker of HSC transdifferentiation.¹⁴ BDL led to an increase in CRP2 expression, reaching a maximum at day 14 after BDL (Figure 6). Most interestingly, DPO treatment diminished the upregulation of CRP2. Furthermore, BDL caused a strong activation of hepatic stellate cells as observed by the 24-fold upregulation of α -SMA mRNA expression at day 2 (control 12.14 ± 3.4) compared with sham-operated animals (sham 0.54 ± 0.29). DPO application significantly prevented the elevation of α -SMA at the early stage after BDL (DPO 3.89 ± 1.28). A three- to fourfold increase in TGF- $\beta 1$ was detected after BDL compared with sham-operated mice with a maximal expression at day 14 after BDL. Treatment with DPO reduced the expression of TGF- $\beta 1$ with a statistically significant difference at day 2 after BDL (Figure 6).

Darbepoetin Improves Survival After BDL in Mice

To test the hypothesis that the pleiotropic profile of DPO results in improved survival, we assessed survival for 7 weeks (Figure 7). Treatment with DPO significantly improved survival in comparison with saline-treated animals after BDL ($P=0.022$).

DISCUSSION

This study presents the following major findings: DPO reduced systemic anemia caused by BDL. Furthermore, treatment with DPO significantly attenuated tissue damage and inhibited the perpetuation of the necro-inflammatory reaction. DPO modulated the expression of profibrotic genes and limited the extent of fibrosis. Finally, treatment with DPO significantly improved survival after BDL.

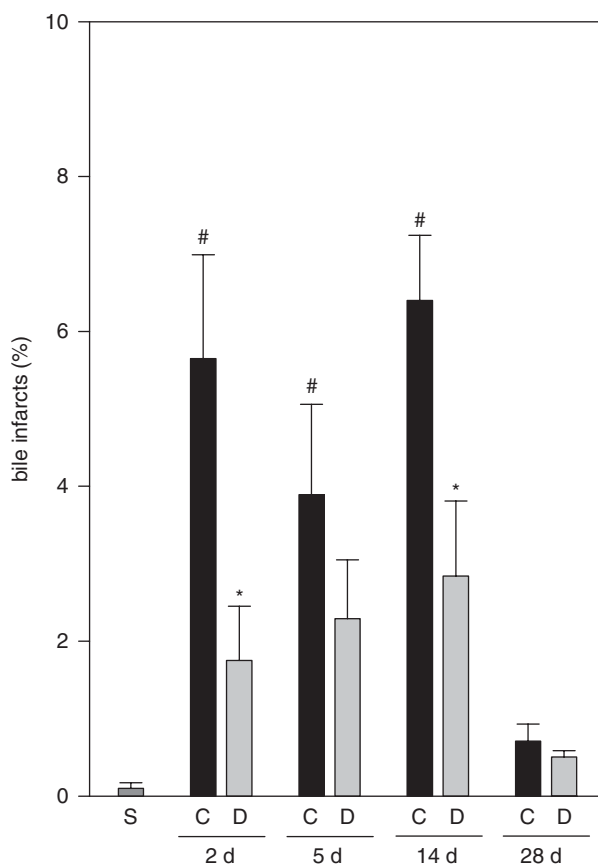
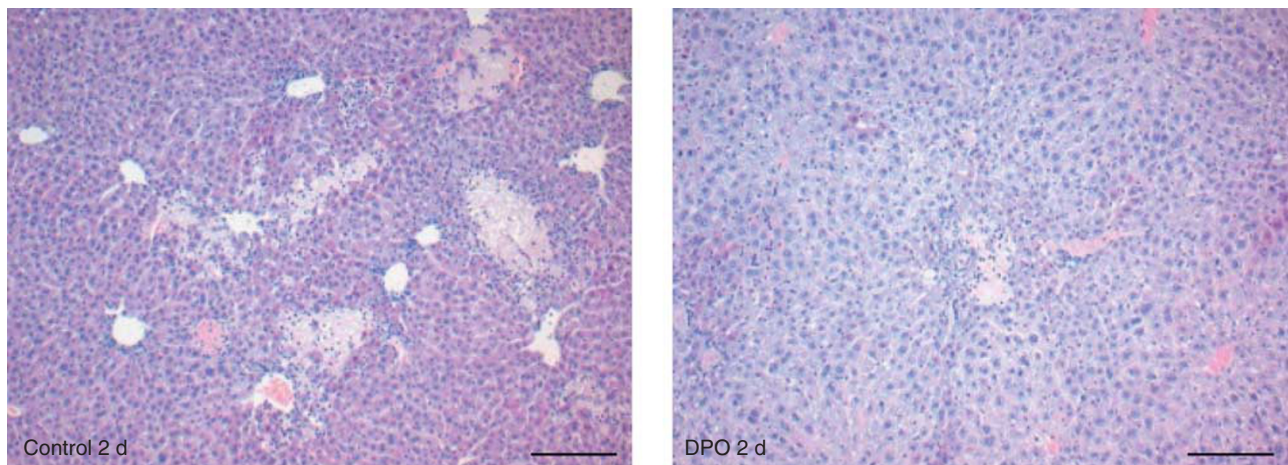


Figure 4 Representative H&E stainings of paraffin-embedded liver sections at day 2 after BDL of a saline-treated control (upper left) and a DPO-treated animal (upper right; bar represents 100 μ m). Quantification of bile infarcts (bottom) in sham-operated mice (S; $n = 3$) and in animals at 2, 5, 14, and 28 days after BDL ($n = 10$ per group and time point) with administration of either 10 μ g/kg body weight darbepoetin- α (D) or physiological saline (C) every third day, beginning 24 h after surgery. Data are given as mean \pm s.e.m. # $P < 0.05$ versus sham (S); * $P < 0.05$ versus control (C) at the respective time points.

Cholestatic liver injury is a dynamic and complex pathophysiological syndrome. The retention of bile salts elicits a toxic response and leads to cellular damage of hepatocytes,¹⁵ which rapidly results in an inflammatory response involving the activation of Kupffer cells and the accumulation of polymorphonuclear leukocytes.^{16–18} In this study, application of DPO markedly decreased the release of hepatocellular

enzymes, bile infarct size, and infiltration of macrophages. The tissue-protective effects of Epo have been reported in different models of acute liver damage. There is ample evidence that Epo reduces the injury caused by ischemia–reperfusion of the liver.^{19–22} Moreover, pre- and post-treatment with DPO in a mouse model of acute liver failure attenuated enzyme release and necrotic cell death as well as

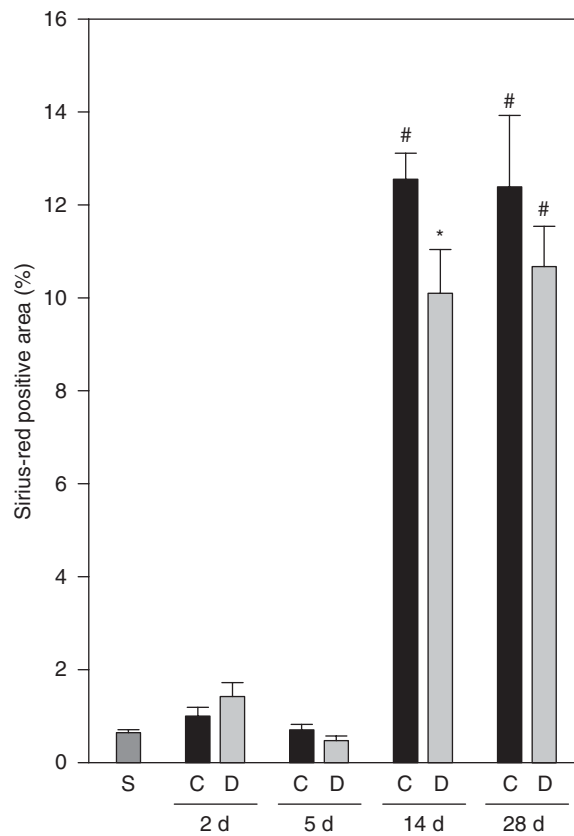
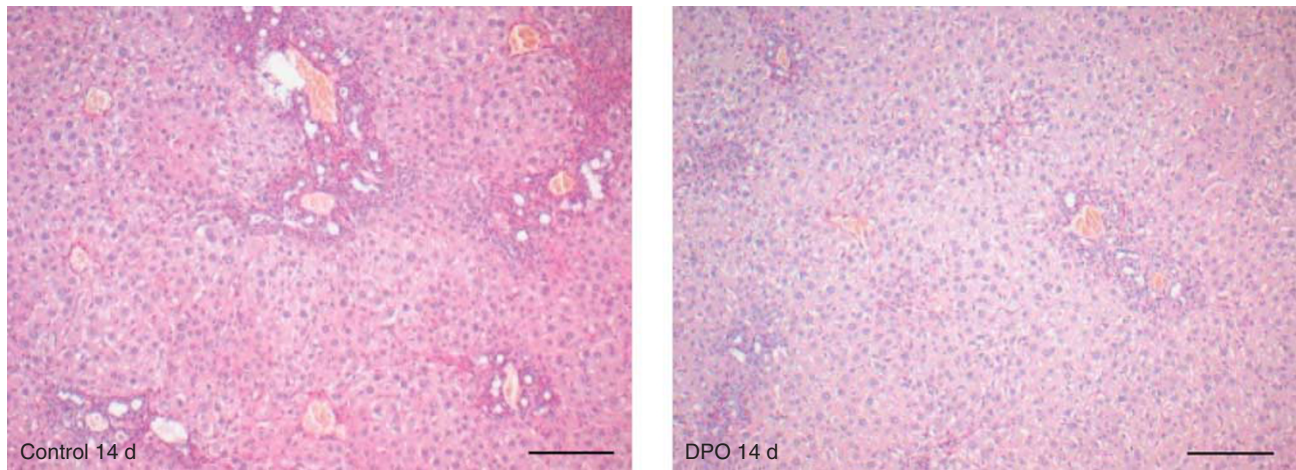


Figure 5 Representative Sirius-red stainings of paraffin-embedded liver tissue sections at day 14 after BDL of a saline-treated control (upper left) and a DPO-treated animal (upper right; bar represents 100 μ m) and quantification of Sirius-red-positive area (bottom) in sham-operated mice (S; $n = 3$) and in animals at 2, 5, 14, and 28 days after BDL ($n = 10$ per group and time point) with administration of either 10 μ g/kg body weight darbepoetin- α (D) or physiological saline (C) every third day, beginning 24 h after surgery. Data are given as mean \pm s.e.m. # $P < 0.05$ versus sham (S); * $P < 0.05$ versus control (C) at the respective time points.

hepatocellular apoptosis.¹¹ Administration of a large dose of erythropoietin after induction of experimental endotoxemia has been shown to improve survival, and was associated with inhibition of apoptosis, nitric oxide production, and tissue hypoxia.²³ In this study, we now show for the first time the tissue-protective effects of an erythropoietin analog in a model of cholestatic liver injury.

Besides the antinecrotic effects, the mechanisms of protection by Epo may involve reduction of apoptotic cell death.^{10,24} To discriminate the protective effects of DPO observed in our study, we analyzed caspase 3 cleavage as a marker of apoptosis. However, we failed to show the enhanced extent of apoptotic liver cell death after BDL (data not shown). These observations confirm the report of

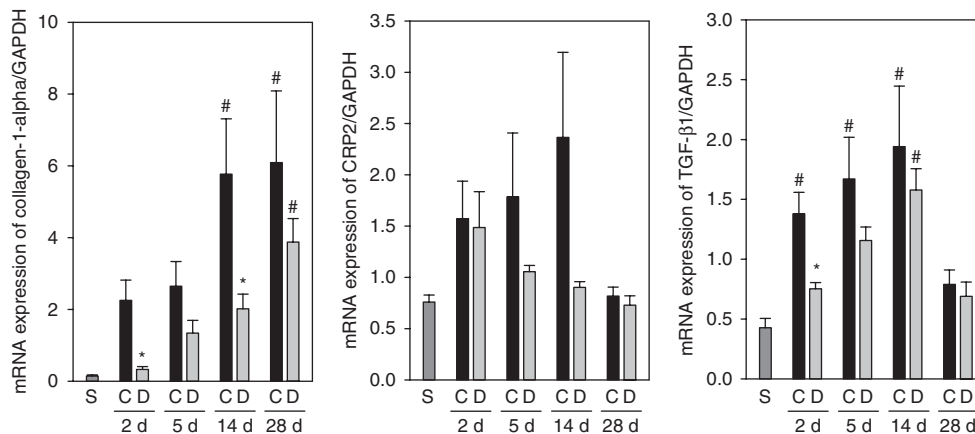


Figure 6 mRNA expression of collagen-(I)- α 1 (left), CRP2 (middle), and TGF- β 1 (right) in liver tissue of sham-operated animals ($n = 4$) and of animals at 2, 5, 14, and 28 days after BDL with administration of either 10 μ g/kg body weight darbepoetin- α (D) or physiological saline (C) every third day, beginning 24 h after surgery ($n = 6$ per group and time point). The expression levels were normalized to that of GAPDH. Data are given as mean \pm s.e.m. # $P < 0.05$ versus sham (S); * $P < 0.05$ versus control (C) at the respective time points.

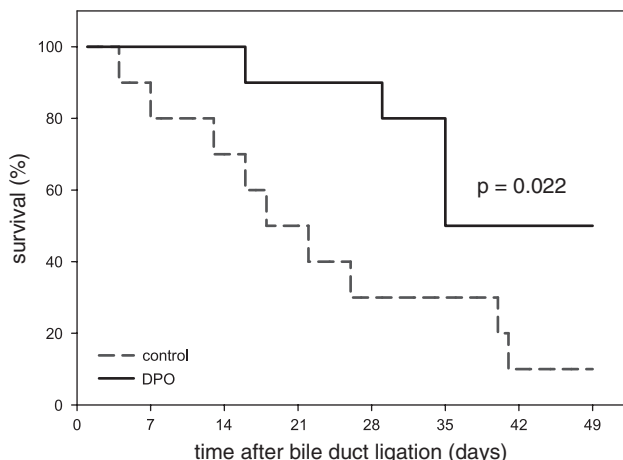


Figure 7 The 7-week survival curve of animals that underwent BDL and were treated with either darbepoetin- α (10 μ g/kg body weight) or physiological saline every third day, beginning 24 h after surgery. Survival log-rank test and *post hoc* comparison; $P = 0.022$ vs control.

Gujral *et al*¹⁸ showing that markers of apoptosis are not increased in mice after BDL. Therefore, we conclude that DPO may prevent tissue damage independently of apoptotic cell death.

It has been shown that hepatic stellate cells are the main source of extracellular matrix production in liver fibrosis.²⁵ The transdifferentiation of the quiescent, fat-storing hepatic stellate cells into myofibroblast-like cells is promoted by a crosstalk between different liver cells. Particularly, Kupffer cells are involved in the activation process of hepatic stellate cells.²⁶ It has been shown that suppressed infiltration of macrophages after liver injury inhibits both activation of stellate cells and development of fibrosis in dimethylnitrosamine-treated rats.¹⁶ Depletion of Kupffer cells with gadolinium chloride after BDL also attenuated liver injury

and reduced fibrogenesis.²⁷ Thus, prevention of macrophage infiltration around the focal infarcts by DPO could be one reason for the decreased activation of hepatic stellate cells in this study.

BDL led to profound changes in liver architecture with typical signs of fibrosis. Collagen deposition was markedly elevated concomitantly with a significant increase in collagen-(I)- α 1 mRNA. Treatment with DPO marginally but significantly reduced both the collagen deposition and the expression of collagen-(I)- α 1 mRNA at day 14 after BDL. The modulation of profibrotic transcripts by DPO as well as the early reduction of necro-inflammation result in delay of progression of cholestatic fibrosis. The hypothesis that this antifibrotic effect could be because of a direct early interaction of DPO with hepatic stellate cells is supported by a study in which Epo treatment suppressed the expression of collagen in angiotensin II-induced activation of cardiac fibroblasts.²⁸ Moreover, recombinant Epo was shown to inhibit the TGF- β -induced epithelial-to-mesenchymal transition in canine kidney epithelial cells.²⁹ Thus, it is reasonable to state that DPO prevents the early epithelial-to-mesenchymal transition in the liver. This transition of epithelial cells and hepatocytes into fibroblasts has been reported as a possible source for extracellular matrix production.^{5,30} It is of interest that the antifibrotic effect of DPO could not be confirmed at 28 days after BDL. The data could support the hypothesis that DPO rather delays than inhibits the profibrotic cascade. On the other hand, it should be noted that data at 28 days after BDL were based on only those animals that survived. The reduced expression levels of profibrotic mediators as well as the markedly reduced area of bile infarcts with lack of progression of fibrosis at day 28 after BDL—as already reported by Georgiev *et al*¹³—are probably because of this positive selection of the mice.

Anemia is a common complication of chronic liver diseases that occurs in approximately 75% of patients.³¹ It has

been shown that a decrease in hemoglobin concentration is an independent factor for the reduced quality of life in patients with cirrhosis.³² Tacke *et al*³³ reported on Epo up-regulation in patients with chronic liver diseases. Thus, the exogenous application with respect to endogenously increased Epo levels may appear as a discrepancy. However, Siciliano *et al*³⁴ suggested an impaired EPO response in patients with liver cirrhosis. Moreover, Bruno *et al*³⁵ showed that an increase in Epo in patients with chronic liver diseases is lower than that observed in patients with iron-deficiency anemia and appears blunted and inadequate in comparison to the degree of anemia. The results of this study show that DPO application effectively reduces anemia in mice. The application of recombinant Epo analogs might therefore be considered to be reasonable.

It is of interest that different studies have reported a link between hypoxia and liver fibrosis, including TGF- β -dependent⁸ and -independent pathways.⁷ Particularly, HIF-1 α is involved in the regulation of different profibrotic genes,³⁶ and HIF-1 α knockout mice showed a significantly lower expression of collagen type I and α -SMA compared with wild-type controls after BDL.⁶ Furthermore, HIF-1 α has been shown to promote experimental renal fibrosis.³⁷ Our investigations show an upregulation of HIF-1 α in liver tissue after BDL. Treatment with DPO was sufficient to prevent the upregulation of HIF-1 α and this may partially mediate the antifibrotic effect. It is of interest that we observed an upregulation of HIF-1 α , especially in the area of bile infarcts. The formation of bile infarcts is not fully understood. Our results encourage us to hypothesize that besides the toxicity of the bile acids, a disruption in the perfusion leading to hypoxia and necrosis is involved in this process. Cholestasis might be associated with impaired microcirculation of the liver with a lack of sinusoidal perfusion and increased leukocyte recruitment. Erythropoietin has been shown to improve the microcirculatory parameters. Therefore, the salutary effects of DPO in our study might be partially mediated by the improved perfusion of the liver tissue leading to decreased necrosis.

Taken together, treatment with DPO reduces the acute cholestatic tissue damage, attenuates the overexpression of profibrotic genes, delays the progression of fibrosis, and significantly improves survival. Our investigations suggest that DPO, which is a clinically well-established compound, could be an efficient therapeutic option for patients with cholestatic liver diseases.

ACKNOWLEDGEMENT

We thank Berit Blendow, Doris Butzlaff, Dorothea Frenz, and Maren Nerowski (Institute for Experimental Surgery, University of Rostock) for excellent technical assistance. This work was supported in part by the Deutsche Forschungsgemeinschaft, Bonn-Bad Godesberg, Germany (Vo 450/10-1), by the Bundesministerium für Bildung und Forschung, Germany (01GN0986), and by the Ministry of Education, Research and Culture Mecklenburg-Vorpommern, Schwerin, Germany (UR 08 008).

DISCLOSURE/CONFLICT OF INTEREST

The authors declare no conflict of interest.

1. Poupon R, Chazouilleres O, Poupon RE. Chronic cholestatic diseases. *J Hepatol* 2000;32(1 Suppl):129–140.
2. Hofmann AF. Cholestatic liver disease: pathophysiology and therapeutic options. *Liver* 2002;22(Suppl 2):14–19.
3. Rodriguez-Garay EA. Cholestasis: human disease and experimental animal models. *Ann Hepatol* 2003;2:150–158.
4. Kountouras J, Billing BH, Scheuer PJ. Prolonged bile duct obstruction: a new experimental model for cirrhosis in the rat. *Br J Exp Pathol* 1984;65:305–311.
5. Gressner OA, Weiskirchen R, Gressner AM. Evolving concepts of liver fibrogenesis provide new diagnostic and therapeutic options. *Comp Hepatol* 2007;6:7.
6. Moon JO, Welch TP, Gonzalez FJ, *et al*. Reduced liver fibrosis in hypoxia-inducible factor-1[alpha]-deficient mice. *Am J Physiol Gastrointest Liver Physiol* 2009;296:G582–G592.
7. Corpechot C, Barbu V, Wendum D, *et al*. Hypoxia-induced VEGF and collagen I expressions are associated with angiogenesis and fibrogenesis in experimental cirrhosis. *Hepatology* 2002;35:1010–1021.
8. Jeong WI, Do SH, Yun HS, *et al*. Hypoxia potentiates transforming growth factor-beta expression of hepatocyte during the cirrhotic condition in rat liver. *Liver Int* 2004;24:658–668.
9. Chatterjee PK. Pleiotropic renal actions of erythropoietin. *Lancet* 2005;365:1890–1892.
10. Brines M, Cerami A. Erythropoietin-mediated tissue protection: reducing collateral damage from the primary injury response. *J Intern Med* 2008;264:405–432.
11. Le Minh K, Klemm K, Abshagen K, *et al*. Attenuation of inflammation and apoptosis by pre- and posttreatment of darbepoetin-alpha in acute liver failure of mice. *Am J Pathol* 2007;170:1954–1963.
12. Sasu BJ, Hartley C, Schultz H, *et al*. Comparison of epoetin alfa and darbepoetin alfa biological activity under different administration schedules in normal mice. *Acta Haematol* 2005;113:163–174.
13. Georgiev P, Jochum W, Heinrich S, *et al*. Characterization of time-related changes after experimental bile duct ligation. *Br J Surg* 2008;95:646–656.
14. Salguero Palacios R, Roderfeld M, Hemmann S, *et al*. Activation of hepatic stellate cells is associated with cytokine expression in thioacetamide-induced hepatic fibrosis in mice. *Lab Invest* 2008;88:1192–1203.
15. Schmucker DL, Ohta M, Kanai S, *et al*. Hepatic injury induced by bile salts: correlation between biochemical and morphological events. *Hepatology* 1990;12:1216–1221.
16. Imamura M, Ogawa T, Sasaguri Y, *et al*. Suppression of macrophage infiltration inhibits activation of hepatic stellate cells and liver fibrogenesis in rats. *Gastroenterology* 2005;128:138–146.
17. Saito JM, Maher JJ. Bile duct ligation in rats induces biliary expression of cytokine-induced neutrophil chemoattractant. *Gastroenterology* 2000;118:1157–1168.
18. Gujral JS, Liu J, Farhood A, *et al*. Reduced oncotic necrosis in Fas receptor-deficient C57BL/6J-lpr mice after bile duct ligation. *Hepatology* 2004;40:998–1007.
19. Hochhauser E, Pappo O, Ribakovskiy E, *et al*. Recombinant human erythropoietin attenuates hepatic injury induced by ischemia/reperfusion in an isolated mouse liver model. *Apoptosis* 2008;13:77–86.
20. Schmeding M, Hunold G, Ariyakhagorn V, *et al*. Erythropoietin reduces ischemia-reperfusion injury after liver transplantation in rats. *Transpl Int* 2009;22:738–746.
21. Shimoda M, Sawada T, Iwasaki Y, *et al*. Erythropoietin strongly protects the liver from ischemia-reperfusion injury in a pig model. *Hepatogastroenterology* 2009;56:470–475.
22. Yilmaz S, Ates E, Tokyol C, *et al*. The protective effect of erythropoietin on ischaemia/reperfusion injury of liver. *HPB (Oxford)* 2004;6:169–173.
23. Aoshiba K, Onizawa S, Tsuji T, *et al*. Therapeutic effects of erythropoietin in murine models of endotoxin shock. *Crit Care Med* 2009;37:889–898.
24. Bernhardt WM, Eckardt KU. Physiological basis for the use of erythropoietin in critically ill patients at risk for acute kidney injury. *Curr Opin Crit Care* 2008;14:621–626.

25. Friedman SL, Roll FJ, Boyles J, *et al*. Hepatic lipocytes: the principal collagen-producing cells of normal rat liver. *Proc Natl Acad Sci USA* 1985;82:8681–8685.
26. Gressner AM, Lotfi S, Gressner G, *et al*. Synergism between hepatocytes and Kupffer cells in the activation of fat storing cells (perisinusoidal lipocytes). *J Hepatol* 1993;19:117–132.
27. Canbay A, Feldstein AE, Higuchi H, *et al*. Kupffer cell engulfment of apoptotic bodies stimulates death ligand and cytokine expression. *Hepatology* 2003;38:1188–1198.
28. Zhang XJ, Ma YX, Wen Y, *et al*. Erythropoietin suppresses the expressions of TGF-beta1 and collagen in rat cardiac fibroblasts induced by angiotensin II. *Zhonghua Xin Xue Guan Bing Za Zhi* 2008;36:636–640.
29. Park SH, Choi MJ, Song IK, *et al*. Erythropoietin decreases renal fibrosis in mice with ureteral obstruction: role of inhibiting TGF-beta-induced epithelial-to-mesenchymal transition. *J Am Soc Nephrol* 2007;18:1497–1507.
30. Wallace K, Burt AD, Wright MC. Liver fibrosis. *Biochem J* 2008;411:1–18.
31. Gonzalez-Casas R, Jones EA, Moreno-Otero R. Spectrum of anemia associated with chronic liver disease. *World J Gastroenterol* 2009;15:4653–4658.
32. Les I, Doval E, Flavia M, *et al*. Quality of life in cirrhosis is related to potentially treatable factors. *Eur J Gastroenterol Hepatol* 2010;22:221–227.
33. Tacke F, Schoffski P, Luedde T, *et al*. Analysis of factors contributing to higher erythropoietin levels in patients with chronic liver disease. *Scand J Gastroenterol* 2004;39:259–266.
34. Siciliano M, Tomasello D, Milani A, *et al*. Reduced serum levels of immunoreactive erythropoietin in patients with cirrhosis and chronic anemia. *Hepatology* 1995;22(4 Pt 1):1132–1135.
35. Bruno CM, Neri S, Sciacca C, *et al*. Plasma erythropoietin levels in anaemic and non-anaemic patients with chronic liver diseases. *World J Gastroenterol* 2004;10:1353–1356.
36. Higgins DF, Kimura K, Iwano M, *et al*. Hypoxia-inducible factor signaling in the development of tissue fibrosis. *Cell Cycle* 2008;7:1128–1132.
37. Kimura K, Iwano M, Higgins DF, *et al*. Stable expression of HIF-1alpha in tubular epithelial cells promotes interstitial fibrosis. *Am J Physiol Renal Physiol* 2008;295:F1023–F1029.